Extensive Throughput Enhancement For 5G Enabled UAV Swarm Networking

Jian Wang, Yongxin Liu, Shuteng Niu, and Houbing Song, Senior Member, IEEE

Abstract—The ubiquitous deployment of 5G New Radio (5G NR) accelerates the evolution in many fields. With the enhancement of 5G NR, Unmanned Aerial Vehicle (UAV) swarm networking can gain more flexibility, reliability, and elasticity to assist residents or workers to finish missions of high complexity and risks remotely. The beamforming of 5G NR can improve the accuracy and the flexibility of connections between the mobile devices. With a high throughput guaranteed in the UAV swarm networking, the remote can deliver specific instructions with the high accuracy of requirement. Further, a reliable and high volume throughput assures multiple UAV swarm networking can exchange information to collaborate and cooperate underneath different mission allocations. In this paper, we propose a cell wall paradigm to escalate the flexibility and the throughput for the heterogeneous 5G enabled UAV swarm networking. With construction of cell wall, we formulate and summarize the throughput optimization into capacity maximal problem to achieve the max-min throughput. Thereafter, we implement an optimal edge coloring solution with the upper bound and the lower bound of color selection to schedule the orders of active links. Based on the optimal scheduling for each separate networking, we focus on the balance of the inter and intra active links to mitigate collisions on the UAVs to strengthen the throughput of UAV swarm networking for the collaboration and corporation of the heterogeneous UAV swarms on a large scale. The evaluation shows the optimal edge coloring approach can improve the throughput for UAV swarm networking at 73.8% maximally. With the optimal setting of $t_s = 0.01s$ and $t_g = 0.01s$, we can achieve the optimal throughput for the collaboration of the heterogeneous UAV swarms globally.

Keywords-UAV swarm networking, Beamforming, 5G New Radio, Cellular networking, Throughput optimization

I. INTRODUCTION

A. Motivation

The compact and affordable of advantages make the next generation Node Base station (gNB) of 5G New Radio (5G NR) deploy ubiquitously on a large scale feasible. With the surpassing capacities of 5G NR, massive applications can have access to the Internet which obtain micro-sensors adhering on the human body, self-driving vehicles, Unmanned Aerial Vehicle (UAV) [1] and so on. The assurance of connection derived from 5G NR provides sufficient reliability, flexibility, and efficiency to the evolution of many fields iteratively. Different from the previous cellular networking, 5G NR extends mm-Waves to deliver the packets jointly which provides several tens of throughput than the conventional cellular networking. The emerging applications of beamforming, network slicing, Machine-to-Machine (M2M), and Device-to-Device (D2D) combine to fuel 5G NR to be a scalable and critical factor which can enhance the connections, collaboration, cooperation, integrity and confidentiality for E-health [2], agriculture [3], education [4], etc. The elastic deployment of 5G NR provides the variable scales of applications to satisfy the multiple requirements in different scenarios.

The conventional approaches are based on the hierarchical or the central architectures which could achieve an outstanding controllability with vulnerability to the dynamics of UAV swarms. The hierarchical and the central architectures requires specific UAV in the swarm to afford the gate way services to its peers and other UAV swarms. To provide sufficient throughput of delivery, the specific UAV needs to install extra communication devices and batteries for power consumption.

Jian Wang, Yongxin Liu, Shuteng Niu, and Houbing Song are with the Security and Optimization for Networked Globe Laboratory (SONG Lab), Department of Electrical Engineering and Computer Science, Embry-riddle Aeronautical University, Daytona Beach, FL, 32114 USA

The quality and efficiency of communication is dependent on the specific UAV which is hard to replaced by other peers and vulnerable to the dynamics of UAV swarms. Due to the specific services provider, the specific UAV have to be online to provide the delivery services for the whole UAV swarm [5]. The communication between heterogeneous UAV swarms will crashed once the specific UAV crashed because of power drainage, or connection lost. The specific UAV approaches can be an obstruction to the potential exploitation of 5G NR on the UAV swarm networking on a large scale. The hierarchical and the central architectures are not reliable to the dynamic of UAV swarm in the flight especially in the scenarios where have exact requirements for the reliability and accuracy on the position hovering and micro operations.

A distributed and decentralized architecture of the inter networking construction for heterogeneous UAV swarm networking is imperative. The distributed and decentralized architecture is supposed to exploit the potentials of 5G NR enhanced UAV swarm networking maximally. Due to the flexibility of the distributed and decentralized architecture, UAV swarm networking can be dynamic and flexible to the variation of deployment and the topology changing. Without the specific UAV, the inter connection between heterogeneous UAV swarm networking do not need install the extra communication devices. The peers of UAV swarms can be selected to provide the gate way services once the UAV is qualified and selected. The purchasing and configuration for the specific UAV can be ignored. The whole connection between heterogeneous UAV swarm networking is not dependent on the specific UAV anymore which also strengthens the reliability, flexibility, and security for each UAV swarm. Further, with equal configurations for each UAV in the UAV swarm, the UAV providing the gate way services can be replaced by its peers seamlessly once its power supply is drained; system

2

crashed, or connection is out of range.

Enhanced with 5G NR, UAV swarm networking can have directional connections exactly via beamforming for packets delivery with the minimization of energy consumption and information leakage [6]. With optimal beam steering management, beamforming can execute optimal beams for connections which can reduce the interference derived from other peers. The distributed and decentralized architecture of networking can be constructed with the directional connections and the minimum interference. Based on the massive implementations of Multiple Input and Multiple Output (MIMO), multiple links can be connected with time division and frequency division for the throughput maximization of UAV swarm networking. The extending of 5G NR can provide the distributed and decentralized inter connection of the heterogeneous UAV swarm networking feasibility, flexibility and reliability.

B. Related Work

The surging demands of enhancement on many fields for UAV swarm accelerates the evolution of UAV swarm networking. With a hierarchical game model for optimization of D2D and UAVs, a predictable dynamic matching market can address the UAV selection and time allocation and a congestion game can solve the channel access problem [7]. To address the Slot access for neighboring cooperation in UAV swarms, a self-organized collision discovery mechanism can avoid the unavailable topology information and information exchange to hinder the slot access [8]. Another way [9] to address the access problem, Direction of Arrival (DOA) can provide the relative position and channel gain for estimation and the mixed integer nonlinear programming (MINLP) can enhance the capability of self-recovering. Enabling UAV learning of deployment and association with ground users with maximum sum-rate of networking, a joint optimization of the balance of bandwidth and quality of services, 2D position deployment and altitude allocation is optimized by 'Learn-As-You-Fly'. Firstly, a distributed matching-based association can balance bandwidth allocation and quality of services. Secondly, K-means helps UAVs to address the deployment of UAVs. Finally, game-theoretic approach maximize the limited interference sum-rate [10]. Simultaneously, a deep Q-learning model can determine the optimal link between two UAV nodes and a locally optimal position of UAV can enhance the overall network performance with an optimization algorithm [11]. However, the interference between the ground nodes and UAV swarm networking is critical to the quality of services (QoS). A twophase transmission protocol can leverage cellular networking and D2D networking to mitigate the interference between ground devices and the UAV swarms [12].

To enhance the connectivity, reliability, flexibility of UAV swarm networking, the cellular networking is considered as the most potential approach to integrate the UAV swarm networking into the National Airspace System (NAS) [13]. To reduce the latency of drone cellular-connected UAV users, A fully-fledged drone-based 3D cellular network is proposed to incorporate UAV users and UAVs in different altitudes.

The optimal deployment of UAV base stations to achieve the maximum coverage for ground users [14], [15]. The optimal estimation of distribution for UAV associated ground users and base stations can achieve the minimum can achieve the minimum for 3D cell association. With minimized latency, the optimal uplink sum-rate can enhance the QoS between UAV swarm networking. A cooperative UAV sense-and-send protocol enables UAV-to-X communication. An analysis of cellular networking serving UAV and ground users is based on user and network-level performance [16] and a two spectrum sharing mechanism in [17]. Joint optimization of subchannel allocation and UAV speed is optimized with three sub-problems resolving of UAV-to-network and cellular user subchannel allocation, UAV-to-UAV subchannel allocation and UAV speed [13]. A 3D positioning for the aeraial base stations can the transmit power allocation for all the nodes in uplink, downlink, and the combination of uplink and downlink [18]. Simultaneously, an optimal spectrum sharing strategy can achieve the minimum rate for UAVs and high cellular ground users uplink [17]. With joint optimization of user association, spectrum allocation, and content caching [19], a liquid state machine can predict the users' content request distribution with limited information and deploy UAVs with optimal resource allocation strategies to maximize the serving associations to users with feasible throughput [20].

5G NR enabled UAV swarm networking benefits from Non-Orthogonal Multiple Access (NOMA) which is considered as a promising approach to provide higher receiver power and enhanced spectrum efficiency for mobile users. A Multiple Input Multiple Ouput NOMA (MIMO-NOMA) assists UAV networking [21] to achieve a higher SNR slopes for the mobile users. With tractable analytical upper bounds for Line of Sight (LoS) and Non Line of Sight (NLoS), the interference to the paired NOMA users can be zero. Concurrently, a UAV-assisted NOMA networking leverages UAV and Base Stations (BS) to provide services to the ground users simultaneously with a joint optimization of UAV trajectory and NOMA precoding [22]. The NOMA extends the association to users under the explosive data traffic [23]. To maximize the minimum average rate among ground users for UAV under OMA and NOMA, a formulation of UAV swarm networking with OMA and NOMA is transformed into a tractable problem and solved with penalty dual-decomposition [24]. A user-centric strategy and a UAV-centric strategy can provide analytical expression and enhancement for the coverage of UAV communication in an imperfect Successive Interference Cancellation (ipSIC) scenario [25].

The throughput of UAV swarm networking is critical to the QoS and safety. To reduce the pressure of Small-cell Base Stations (SBS), UAVs are facilitated with caches to assist the offloading request to SBS and improve throughput for video requirement of end mobile users [26]. Joint optimization of UAV deployment, caching placement and user association can maximize the quality of experience (QoE) [27]. A joint optimization of time allocation and position for UAV can maximize uplink throughput for ground users [28] and ground nodes [29]. With minimization of propulsion energy and operation cost, joint optimization of UAV trajectory, sensor node

of wake-up time allocation and transmitting power can achieve the propulsion energy consumption and operation cost [30]. A Swarm A tractable 3D model can evaluate the average downlink of UAV swarm networking with 5G NR and satisfy the requirement of high throughput of UAV networking [31]. To overcome the information leakage and increase the transmission reliability, an optimization for the multi-hop relaying networking [32] can enhance the throughput of UAVs networking with optimized configuration of coding rates, transmit power and required number of hops [33]. With machine learning, the probability of spatial false alarm and spatial missed detection at UAV can formulate the distribution of active UAVs, and assist the stochastic geometry to derive the coverage probability of D2D [34] and UAV networking. A dynamic fly-hover-transmit scheme can determine the UAVs' mobility and transmit power to (Wireless information transfer, wireless energy transfer, and

C. Contributions and Paper Structure

over all ground terminals [35].

In this paper, our contributions are summarized as the follows:

silent) to achieve the UAVs' sum-throughput maximization

- We propose a cell wall paradigm to enhance the flexibility and the throughput for the heterogeneous 5G NR enabled UAV swarm networking. In both full-duplex and half-duplex modes, we formulate and summarize the throughput optimization into capacity maximization to achieve the max-min throughput.
- 2) With implementation of the upper bound and the lower bound, an optimal edge coloring can obtain the optimized scheduling of active links.
- 3) The balance of the inter and intra active links can mitigate collisions on the UAVs to strengthen the throughput of UAV swarm networking globally for the collaboration and corporation of the heterogeneous UAV swarms on a large scale.

The evaluation shows the optimal edge coloring approach can improve the throughput for UAV swarm networking significantly. With the optimal setting of collision mitigation, we can achieve the optimal throughput for the collaboration of the heterogeneous UAV swarms globally.

The paper is organized as follows: Section I illustrates introductions and our contributions. Section II depicts the system model. Section III describes cell wall formulation and the max-min throughput rendering. Section IV maximizes the throughput with edge coloring solving. Section V extends throughput optimization for the heterogeneous UAV swarm networking on a large scale. Section VI presents the evaluation. Section VII concludes the paper.

II. SYSTEM MODEL

We consider a system model (depicted as Fig. 1) consists of a heterogeneous UAV swarm networking that contains multiple heterogeneous UAV swarms. Each UAV is equipped with compact 5G NR devices.

Fig. 1. Collaboration between the heterogeneous UAV swarms

To acquire the location sharing for the UAV swarms, each UAV can obtain other UAVs' location, (x, y, z), with Automatic Dependent Surveillance-Broadcast (ADS-B). Thereafter, the UAV can calculate the distance between its location and other UAVs' with messages derived from ADS-B [36]. The UAV i can obtain the distance between its location to the UAV j:

$$d_{ij} = \sqrt{(x_i - x_j)^2 + (y_i - y_j)^2 + (z_i - z_j)^2}$$
 (1)

Compared with 5G NR transmission range, ADS-B can reach several tens miles which can be considered infinite for the 5G NR transmission limit. The main carriers of ADS-B are 978MHz and 1090MHz which are far away from the carriers of 5G networking. The interference derived from ADS-B to RF beams can be negligible.

A UAV in a swarm is together with many peers of the other swarm in a heterogeneous Time Division Multiple Access (TDMA) cellular networking. Compared with other modulations, TDMA can achieve more flexible access and reliable connections with less interference between different channels. The UAV of the cell wall in each swarm is considered as the backhaul gateway for the UAV of the cell wall in the other swarm. Each UAV is equipped with 5G NR device to generate beams for the connections. The UAV can construct connections once the other UAV is within the range of communication. The receiving signal for the other UAV is denoted as c. The receiving signal of UAV i from the UAV j can be given:

$$c_{ij} = g_{ij}log(1 + \frac{p_j}{10^{PL_{ij}/10\sigma^2}})$$
 (2)

Here, $c_{ij} > 0$ [37], where g_{ij} is direct gain of channel, p_j is transmission power of j, and σ is Gaussian noise distributed with zero mean. PL_{ij} is the path loss between UAV i and UAV j [38], which is given:

$$PL_{ij} = \begin{cases} 20log_{10}(d_{ij}) + 20log_{10}(f_{ij}) + \eta_{LoS} \\ 20log_{10}(d_{ij}) + 20log_{10}(f_{ij}) + \eta_{NLoS} \end{cases}$$
(3)

where d_{ij} is the distance between UAV i and UAV j and f_{ij} is the frequency of UAV j adopts. η_{LoS} and η_{NLoS} are the

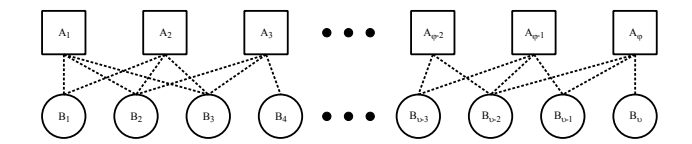


Fig. 2. Cell wall between swarm A and swarm B

attenuation for LoS and NLoS respectively. LoS is deployed within the UAV swarm networking and NLoS is deployed for the connections between the heterogeneous UAV swarms.

For the heterogeneous UAV swarm networking, connection time is not static which may vary according to mission assignment. An optimal throughput for collaboration between heterogeneous UAV swarm networking in each connection frame can escalate QoS for the mission complement. With TDMA, the collaboration time, denoted as \mathcal{T} , can be divided into multiple connection frames (denoted as \mathcal{F}). Thereafter, \mathcal{F} can be divided into multiple unit time scales, 1. The unit time scale can be scheduled into N slots t, where $N \geq 1$. The k_{th} slot is defined as t_k which follows the constraint:

$$\sum_{k=1}^{N} t_k \le 1 \tag{4}$$

Here, $1 \geq t_k \geq 0$. Further, in k_{th} slot, a set of beams between swarm A, swarm B, swarm C can be constructed to deliver messages between swarm A and swarm C. The connections generated between swarm A and swarm B can be denoted as \mathcal{E}_{AB} . The connections generated between swarm B and swarm C can be denoted as \mathcal{E}_{BC} . The valid connections of \mathcal{E}_{AB} and \mathcal{E}_{BC} can be active at the i_{th} slot. The active selections for \mathcal{E}_{AB} and \mathcal{E}_{BC} are \mathcal{E}_{AB} and \mathcal{E}_{BC} . We assume there are \mathcal{M} and \mathcal{N} connections for \mathcal{E}_{AB} and \mathcal{E}_{BC} . Here, $\mathcal{E}_{AB} = \{0,1\}^V$ and $\mathcal{E}_{BC} = \{0,1\}^W$. $\mathcal{E}_{AB} = \{0,1\}^V$.

$$\sum_{k=1}^{N} t_k \times \mathcal{S}_{AB} \le 1 \tag{5a}$$

$$\sum_{k=1}^{N} t_k \times \mathcal{S}_{BC} \le 1 \tag{5b}$$

III. CELL WALL CONSTRUCTION

In nature, cells communicate with each other with the assistance of cell walls which has wider flexibility and reliability than the point to point connections. The conventional approaches require some specific UAVs with outstanding configurations to provide the gateway services for the communication between a heterogeneous UAV swarm networking. With ADS-B, UAV can obtain the location of other UAVs in the different swarms and determine whether the UAV is within the range of the valid connections.

The abstract architectures of the cell wall of swarm A, swarm B, and swarm C are depicted as Fig. 2 and Fig. 3. We assume that there are φ UAVs in swarm A and ν UAVs in swarm B consisting of the cell wall for the connections for swarm A and swarm B, and there are ω UAVs and λ UAVs consisting of the cell wall for the connections for swarm B and swarm C. With constructed cell walls among swarm A,

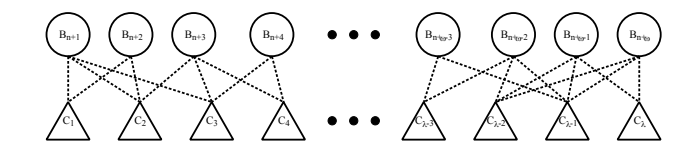


Fig. 3. Cell wall between swarm B and swarm C

swarm B and swarm C, we can have the throughput arrays for the cell walls of swarm A and swarm B (denoted as CW_1) and the cell wall of swarm B and swarm C (denoted as CW_2).

For the full-duplex scenarios, we can have C_{CW_1} and C_{CW_2} as (6) and (7).

$$C_{CW_1} = \begin{pmatrix} c_{11} & \cdots & c_{1\varphi} \\ \vdots & \ddots & \vdots \\ c_{\nu 1} & \cdots & c_{\nu \varphi} \end{pmatrix}$$
 (6)

$$C_{CW_2} = \begin{pmatrix} c_{[n+1]1} & \cdots & c_{[n+1]\lambda} \\ \vdots & \ddots & \vdots \\ c_{[n+\omega]1} & \cdots & c_{[n+\omega]\lambda} \end{pmatrix}$$
(7)

In the full-duplex scenario, the optimal throughput for CW_1 and CW_2 is (8). And the beams between cell wall can not occur collision which means each two beams can share no same UAVs in the connections.

$$\max \sum c_{CW_1} + \sum c_{CW_2} \tag{8a}$$

$$S. T. i \neq j \neq l \neq m, \forall c_{ij}, \forall c_{lm} \in C_{CW_1}$$
(8b)

$$i \neq j \neq l \neq m, \forall c_{ij}, \forall c_{lm} \in C_{CW_2}$$
 (8c)

Based on the linear computation, we can divide (8) into two independent optimizations, which can be (9) and (10):

$$\max \sum_{k=1}^{N} c_{C_{CW_1}} \times t_k \times \mathcal{S}_{AB}$$
 (9a)

S. T.
$$i \neq j \neq l \neq m, \forall c_{ij}, \forall c_{lm} \in C_{CW_1}$$
 (9b)

$$\max \sum_{k=1}^{N} c_{C_{CW_2}} \times t_k \times \mathcal{S}_{BC}$$
 (10a)

S. T.
$$i \neq j \neq l \neq m, \forall c_{ij}, \forall c_{lm} \in C_{CW_2}$$
 (10b)

For the half-duplex scenarios, the upload links are different from the download links which the throughput is different. Thus, we have \hat{C}_{CW_1} and \hat{C}_{CW_2} which are (11) and (12). To specify swarm A, swarm B, and swarm C in the half-duplex scenarios and mitigate the confusion, we use the upper \star to mark swarm A in CW_1 and the upper \star to mark swarm C in CW_2 .

$$\hat{C}_{CW_{1}} = \begin{pmatrix} c_{1^{*}1} & \cdots & c_{1^{*}\varphi} & 0 & \cdots & 0 \\ \vdots & \ddots & \vdots & \vdots & \ddots & \vdots \\ c_{\nu^{*}1} & \cdots & c_{\nu^{*}\varphi} & 0 & \cdots & 0 \\ 0 & \cdots & 0 & c_{11^{*}} & \cdots & c_{\varphi^{1^{*}}} \\ \vdots & \ddots & \vdots & \vdots & \ddots & \vdots \\ 0 & \cdots & 0 & c_{1\nu^{*}} & \cdots & c_{\varphi\nu^{*}} \end{pmatrix}$$
(11)

$$\hat{C}_{CW_{2}} = \begin{pmatrix} c_{[n+1]1^{*}} & \dots & c_{[n+1]\lambda^{*}} & 0 & \dots & 0 \\ \vdots & \ddots & \vdots & \vdots & \ddots & \vdots \\ c_{[n+\omega]1^{*}} & \dots & c_{[n+\omega]\lambda^{*}} & 0 & \dots & 0 \\ 0 & \dots & 0 & c_{1^{*}[n+2]} & \dots & c_{\lambda^{*}[n+2]} \\ \vdots & \ddots & \vdots & \vdots & \ddots & \vdots \\ 0 & \dots & 0 & c_{1^{*}[n+\omega]} & \dots & c_{\lambda^{*}[n+\omega]} \end{pmatrix}$$
(12)

In the half-duplex scenario, the optimal throughput for CW_1 and CW_2 is (13). And the beams between cell wall can not occur collision which means each two beams can share no same UAVs in the same swarm in the connections.

$$\max \sum c_{CW_1} + \sum c_{CW_2} \tag{13a}$$

S. T.
$$i \neq j$$
, $l \neq m, \forall c_{ij}, \forall c_{lm} \in \hat{C}_{CW_1}$ (13b)

$$i \neq j, \ l \neq m, \forall c_{ij}, \forall c_{lm} \in \hat{C}_{CW_2}$$
 (13c)

To simplify \hat{C}_{CW_1} , we decompose \hat{C}_{CW_1} into $\hat{C}_{CW_{1A}}$ and $\hat{C}_{CW_{1B}}$.

$$\hat{C}_{CW_{1A}} = \begin{pmatrix} c_{1\star_1} & \cdots & c_{1\star_{\varphi}} \\ \vdots & \ddots & \vdots \\ c_{\nu\star_1} & \cdots & c_{\nu\star_{\varphi}} \end{pmatrix}$$
(14)

$$\hat{C}_{CW_{1B}} = \begin{pmatrix} c_{11^{\star}} & \cdots & c_{\varphi_{1^{\star}}} \\ \vdots & \ddots & \vdots \\ c_{1\nu^{\star}} & \cdots & c_{\varphi_{\nu^{\star}}} \end{pmatrix}$$
(15)

Based $\hat{C}_{CW_{1A}}$ (14) and $\hat{C}_{CW_{1B}}$ (15), \hat{C}_{CW_1} can be (16):

$$\hat{C}_{CW_1} = \begin{pmatrix} \hat{C}_{CW_{1A}} & 0\\ 0 & \hat{C}_{CW_{1B}} \end{pmatrix}$$
 (16)

Based on (16), the optimization of (9) can be:

$$\max \left(\sum_{k=1}^{N} c_{CW_{1A}} + \sum_{k=1}^{N} c_{CW_{1B}} \right) \times t_k \times S_{AB}$$
 (17a)

S. T.
$$i \neq j \neq l \neq m, \forall c_{ij}, \forall c_{lm} \in \hat{C}_{CW_{1,4}}$$
 (17b)

$$i \neq j \neq l \neq m, \forall c_{ij}, \forall c_{lm} \in \hat{C}_{CW_{1B}}$$
 (17c)

Similar with (9) and (10), (17) can be divided into (18) and (19):

$$\max \sum_{k=1}^{N} c_{CW_{1A}} \times t_k \times \mathcal{S}_{AB}$$
 (18a)

S. T.
$$i \neq j \neq l \neq m, \forall c_{ij}, \forall c_{lm} \in \hat{C}_{CW_{1A}}$$
 (18b)

$$\max \sum_{k=1}^{N} c_{CW_{1B}} \times t_k \times \mathcal{S}_{AB}$$
 (19a)

S. T.
$$i \neq j \neq l \neq m, \forall c_{ij}, \forall c_{lm} \in \hat{C}_{CW_{1B}}$$
 (19b)

Similar with \hat{C}_{CW_1} , we decompose \hat{C}_{CW_2} into $\hat{C}_{CW_{2B}}$ and $\hat{C}_{CW_{2C}}$.

$$\hat{C}_{CW_{2B}} = \begin{pmatrix} c_{[n+1]1^*} & \dots & c_{[n+1]\lambda^*} \\ \vdots & \ddots & \vdots \\ c_{[n+\omega]1^*} & \dots & c_{[n+\omega]\lambda^*} \end{pmatrix}$$
(20)

$$\hat{C}_{CW_{2C}} = \begin{pmatrix} c_{1^*[n+2]} & \cdots & c_{\lambda^*[n+2]} \\ \vdots & \ddots & \vdots \\ c_{1^*[n+\omega]} & \cdots & c_{\lambda^*[n+\omega]} \end{pmatrix}$$
(21)

Based $\hat{C}_{CW_{2B}}$ (20) and $\hat{C}_{CW_{2C}}$ (21), $\hat{C}_{CW_{2}}$ can be (22):

$$\hat{C}_{CW_2} = \begin{pmatrix} \hat{C}_{CW_{2B}} & 0\\ 0 & \hat{C}_{CW_{2C}} \end{pmatrix}$$
 (22)

Based on (22), the optimization of (10) can be:

$$\max \left(\sum_{k=1}^{N} c_{CW_{2B}} + \sum_{k=1}^{N} c_{CW_{2C}} \right) \times t_k \times \mathcal{S}_{BC}$$
 (23a)

S. T.
$$i \neq j \neq l \neq m, \forall c_{ij}, \forall c_{lm} \in \hat{C}_{CW_{2R}}$$
 (23b)

$$i \neq j \neq l \neq m, \forall c_{ij}, \forall c_{lm} \in \hat{C}_{CW_{2C}}$$
 (23c)

Similar with (18) and (19), (23) can be divided into (24) and (25).

$$\max \sum_{k=1}^{N} c_{CW_{2B}} \times t_k \times \mathcal{S}_{BC}$$
 (24a)

S. T.
$$i \neq j \neq l \neq m, \forall c_{ij}, \forall c_{lm} \in \hat{C}_{CW_{2B}}$$
 (24b)

$$\max \sum_{k=1}^{N} c_{CW_{2C}} \times t_k \times \mathcal{S}_{BC}$$
 (25a)

S. T.
$$i \neq j \neq l \neq m, \forall c_{ij}, \forall c_{lm} \in \hat{C}_{CW_{2C}}$$
 (25b)

With decomposition of (16) and (22), we have (18), (19), (24) and (25) which have a similar formation of (9) and (10). We conclude them as (26), and these optimizations can be solved with the solution of (26). The only differences are the scale and the efficiency of optimization which are variable according to the generated links.

$$\max \sum_{k=1}^{N} c \times t_k \times \mathcal{S} \tag{26a}$$

$$S. T. i \neq j \neq l \neq m, \forall c_{ij}, \forall c_{lm} \in C$$
 (26b)

Here, $C = \{C_{CW_1}, C_{CW_2}, \hat{C}_{CW_1}, \hat{C}_{CW_2}\}$. We fix t_k and \mathcal{S} , and search c for the optimization and the achievement of the max-min throughput without optimization of scheduling. We adopt the greedy algorithm (shown as Algorithm 1) to find the max-min capacity of the links for each cell wall with fixed time allocation.

Algorithm 1: Render the max-min throughput σ

IV. MAXIMIZATION THROUGHPUT SCHEDULING

Based on the max-min throughput for each cell wall, we can achieve an optimization of the fixed beam connections which are not elastic and reliable to the dynamic of UAV swarms. The collision also includes interference between neighbor beams in the same time slot t_k with the same frequency allocation.

In the following part, we will focus on the time allocation optimization t_k to enhance the throughput of UAV swarm networking with the maximum connections and the minimum collisions between beams. Both situations of half-duplex and full-duplex have the same issues of incidents of enabled links. Especially, the full-duplex situation may suffer more serious incidents.

To mitigate the collisions between different beams, some beam connections have to be aborted with a greedy algorithm in section III. To address the problem of time allocation, we map the connections of CW_1 and CW_2 into two directed graphs G_1 and G_2 . Each UAV is denoted as a vertex (\mathcal{V}) in the graph and the connection between different UAVs are denoted as an edge (\mathcal{E}) of graph. Thus, we have $G_1 = (\mathcal{V}_{\varphi+\nu}, \ \mathcal{E}_{\varphi+\nu})$ and $G_2 = (\mathcal{V}_{\omega+\lambda}, \ \mathcal{E}_{\omega+\lambda})$. Due to the conclusion of (26), the scheduling with multiple connections in the multiple time slots can be solved with the similar solution. We focus on the resolving of (26), and extend its solution to the subtle optimizations. To specific each active time, we install t_g for $\lceil \frac{t_k}{t_g} \rceil - 1$ links and the rest links assigned to the time of $mod(t_k, t_g)$. Here, mod is modulo operation in mathematics. Next, we formulate the optimization into (27):

$$\max \sum_{i,j=1}^{N} \sum_{q=1}^{P} c_{ij} \times t_g \times \mathcal{S}^*$$
 (27a)

$$S.T. \sum t_g \le t_k \tag{27b}$$

We assume there are P-1 sections can be derived from t_k with the length of t_g and 1 section for $mod(t_k, t_g)$. We can have (28):

$$t_{k} = (\lceil \frac{t_{k}}{t_{g}} \rceil - 1)t_{g} + mod(t_{k}, t_{g})$$

$$\leq (\lceil \frac{t_{k}}{t_{g}} \rceil - 1)t_{g} + t_{g}$$

$$\leq Pt$$
(28)

$$\sum_{k=1}^{N} t_k \le \sum_{k=1}^{N} \lceil \frac{t_k}{t_g} \rceil t_g \le \sum_{k=1}^{N} Pt_g$$
 (29)

To schedule the time allocation into a unit time, 1, we need to readjust the t_g to satisfy all valid links active in the desired frame. According to (29), if $\sum_{k=1}^N Pt_g > 1$, we need to readjust t_g to be shrink into the unit time. The shrinkage factor of each link time is α which can guarantee $\alpha \sum_{k=1}^N Pt_g = 1$. We can have $\alpha = \frac{1}{\sum_{k=1}^N Pt_g}$. The updated link allocation time $t_g^* = \alpha t_g$. Optimization of (27) can be modified to (30):

$$\max \sum_{ij}^{N} \sum_{g=1}^{P} c_{ij} \times t_g^{\star} \times \mathcal{S}^{*}$$
 (30a)

$$S.T. \sum t_g^{\star} = t_k \tag{30b}$$

Otherwise, $\sum_{k=1}^{N} Pt_g \leq 1$, we can keep t_g unchanged.

With the optimized time allocation, t_g , for links, we can separate the links with P sections. With the directed graph $G = \{G1, G2\}$, we can use edge coloring to allocate orders for each link with the minimum collision for the activation duration. To achieve the optimum edge coloring solution for G, we first need to render the maximum mode degree of G. With the algorithm proposed in [39], we can obtain the degree of G in (31):

$$\Delta(G) = \sum_{k=1}^{\mathcal{N}} \lceil \frac{t_k}{t_g} \rceil < \sum_{k=1}^{\mathcal{N}} (\frac{t_k}{t_g} + 1)$$

$$\leq \frac{t_g(\mathcal{V}_G - 1) + 1}{t_g}$$
(31)

Here, V_G is the vertex of G. For the multigraphs, the upper bound of colors used is $3\lceil \frac{\triangle G}{2} \rceil$ which is (32):

$$P_{upper} \leq 3 \cdot \lceil \frac{\Delta G}{2} \rceil$$

$$= 3 \cdot \lceil \frac{t_g(\mathcal{V}_G - 1) + 1}{2 \cdot t_g} \rceil$$
(32)

Furthermore, based on the upper bound we achieved in (32), we can extend the lower bound of G to accelerate the optimum of searching. With induction presented in [40], we can have the lower bound for G in (33) is:

$$P_{lower} \ge \lfloor \frac{\triangle G}{2} \rfloor$$

$$= \lfloor \frac{t_g(\mathcal{V}_G - 1) + 1}{2} \rfloor$$
(33)

With rendering of P_{upper} and P_{lower} in (32) and (33), we can start searching from the lower bound and readjust until there are no collision occurring in G. Here, $P = \{P_{upper}, P_{lower}\}$. To explore the optimum solution, we will calculate the upper bound and the lower bound for the edge coloring of the graph with the counting of vertex and edges. With obtaining the lower bound and the upper bound, we keep the orders of coloring counting when it is lower than the lower bound and recalculate when the order is over the upper bound. The coloring orders is scheduled in S^* which is based on the achievement of S.

V. BALANCE BETWEEN INTER AND INTRA THROUGHPUT

Based on the optimal throughput for each cell wall G_1 and G_2 , we can have the dependent optimization of G_1 and G_2 to enhance the throughput between UAV swarms. We assume the networking $\mathcal G$ consists of swarm A (denoted as G_A), swarm B (denoted as G_B), swarm C (denoted as G_C), and two cell walls (G_1 and G_2). The updated scheduling of $\hat{\mathcal S}$ is based on the optimal scheduling of the separated networking including swarm A, swarm B, swarm C, and two cell walls (G_1 and G_2). Based on the achievement in section IV, each networking can be summarized into G and the scheduling can be summarized into $\mathcal S^\star$. $\mathcal G = \{G_A, G_B, G_C, G_1, G_2\}$ and $\hat{\mathcal S} = \{\mathcal S_A^\star, \mathcal S_B^\star, \mathcal S_C^\star, \mathcal S_1^\star, \mathcal S_2^\star\}$. $\mathcal T = \{\mathcal T_A, \mathcal T_B, \mathcal T_C, \mathcal T_1, \mathcal T_2\}$

and $C = \{C_A, C_B, C_C, C_1, C_2\}$. We can have the optimization of (34):

$$\max \mathcal{C} \times \mathcal{T} \times \hat{\mathcal{S}} \tag{34a}$$

S. T.
$$i \neq j \neq l \neq m, \forall c_{ij}, \forall c_{lm} \in \hat{C}_A$$
 (34b)

$$i \neq j \neq l \neq m, \forall c_{ij}, \forall c_{lm} \in \hat{C}_B$$
 (34c)

$$i \neq j \neq l \neq m, \forall c_{ij}, \forall c_{lm} \in \hat{C}_C$$
 (34d)

$$i \neq j \neq l \neq m, \forall c_{ij}, \forall c_{lm} \in \hat{C}_1$$
 (34e)

$$i \neq j \neq l \neq m, \forall c_{ij}, \forall c_{lm} \in \hat{C}_2$$
 (34f)

$$i \neq j \neq l \neq m, \forall c_{ij}, \forall c_{lm} \in \hat{C}_A \cap \hat{C}_1$$
 (34g)

$$i \neq j \neq l \neq m, \forall c_{ij}, \forall c_{lm} \in \hat{C}_B \cap \hat{C}_1$$
 (34h)

$$i \neq j \neq l \neq m, \forall c_{ij}, \forall c_{lm} \in \hat{C}_B \cap \hat{C}_2$$
 (34i)

$$i \neq j \neq l \neq m, \forall c_{ij}, \forall c_{lm} \in \hat{C}_C \cap \hat{C}_2$$
 (34j)

With the maximization of C and T rendering from Section III and Section IV, we can convert the optimization into a maximization of \hat{S} . We adjust the activation order of links to avoid incidents and maximize the throughput reliably. The incidents mitigation can relieve the throughput waste and maintain a good quality of services and communication in real time.

For each networking, G_1 and G_A have achieved the optimal scheduling for the separated networking locally. The collaboration between G_1 and G_A may have collisions for the activation links at the same time slot which can reduce the efficiency and reliability of the information exchange. We focus on the resolving of sharing nodes (denoted as U_N) of G_1 and G_A . To keep the balance between G_1 and G_A , the links (denoted as U_N —) from G_1 to G_A are equal to the links (denoted as U_N+) from G_A to G_1 in the throughput allocation. We can have the optimization (35):

$$\max \sum_{C \subset U_N -} \|\mathcal{C} \times \mathcal{T} \times \hat{\mathcal{S}}\| + \sum_{C \subset U_N +} \|\mathcal{C} \times \mathcal{T} \times \hat{\mathcal{S}}\| \quad (35a)$$

$$S.T. \sum_{C \subset U_N -} \mathcal{C} \times \mathcal{T} \times \hat{\mathcal{S}} + \sum_{C \subset U_N +} \mathcal{C} \times \mathcal{T} \times \hat{\mathcal{S}} = 0 \quad (35b)$$

S.T.
$$\sum_{C \subset U_N -} \mathcal{C} \times \mathcal{T} \times \hat{\mathcal{S}} + \sum_{C \subset U_N +} \mathcal{C} \times \mathcal{T} \times \hat{\mathcal{S}} = 0 \quad (35b)$$

We define the throughput of U_N+ is positive and U_N is negative in the arithmetic. The optimal \hat{S} mainly solve the incidents on U_N . There are two main situations in U_N activation. 1) In time slot of t_g , the active throughput is $\sum c_{ij}$, and c_{ij} are just from one side of U_N+ and U_N- . 2) In time slot of t_q , there are two more active links input and output the same nodes of U_N from both sides. The throughput is $\sum_{c_{ij} \in \{C_{U_N+}, \ C_{U_N-}\}} c_{ij}$. We have the active distribution of c_{U_N} at time slot $t=t_g$:

$$c_{U_N} = \begin{cases} \sum_{c_{ij} \in C_{U_N+}} c_{ij}, \ t = t_g; & (36a) \\ \sum_{c_{ij} \in C_{U_N-}} c_{ij}, \ t = t_g; & (36b) \\ \sum_{c_{ij} \in C_{U_N-}} c_{ij}, \ t = t_g; & (36c) \end{cases}$$

$$\sum_{c_{ij} \in C_{U_N-}} c_{ij}, t = t_g; \qquad (36c)$$

For situation (36a) and (36b), there are no collision occurring in the time slot of t_q , we do not need to obtain the optimization. For situation (36c), we need to optimize the active links to obtain the balance between each networking G_1 and G_A aiming at minimizing incidents at the same time slots. We separate the time slot into smaller time pieces t_s , $\sum_{n=1}^{N} t_s \leq t_g$. Each t_s does not have to be equal in t_g .

$$\max \sum_{n=1}^{N} (\|\sum_{c_{ij} \in c_{U_N+}} c_{ij} \times t_s\| + \|\sum_{c_{ij} \in c_{U_N-}} c_{ij} \times t_s\|) \quad (37a)$$

S.T.
$$\sum_{n=1}^{N} \left(\sum_{c_{ij} \in c_{U_N+}} c_{ij} \times t_s + \sum_{c_{ij} \in c_{U_N-}} c_{ij} \times t_s \right) = 0 \quad (37b)$$

$$\sum_{n=1}^{N} t_s \le t_g \tag{37c}$$

With the optimization of (37), we can achieve the optimal throughput for each node in U_N from bi-directions. Thus, we have the optimal throughput for G_1 and G_A with rendering of $\{t_s\}^N$. For the scheduling of \hat{S} , to put the update time allocation into \hat{S} , we need to re-scale the t_q for fit the time slot with scaling factor of B. $B = \frac{\{t_s\}^N}{t_g} = \{\beta_1, \beta_2, ..., \beta_N\}$. $\hat{\mathcal{S}}^\star = B \cdot \hat{\mathcal{S}} = \{\beta_1 \cdot \hat{\mathcal{S}}_1, \beta_2 \cdot \hat{\mathcal{S}}_2, \beta_3 \cdot \hat{\mathcal{S}}_3, ..., \beta_N \cdot \hat{\mathcal{S}}_N\}$. Based on the artifactor of $\hat{\mathcal{S}}_1$ and $\hat{\mathcal{S}}_2$ and $\hat{\mathcal{S}}_3$ on the optimal throughput of $G_1 + G_A$, we can consider $G_1 + G_A$ as a new networking, and extend it with connection of G_B . Similarly, we can extend the networking with the combination of G_2 and G_C sequentially. Eventually, we can have the optimal throughput for the networking of \mathcal{G} with the scheduling of \hat{S} .

Based on the achievement of throughput optimization, the throughput optimization can be extended and implemented into multiple UAV swarm networking (3 more) with obtaining flexibility and reliability of networking on the collaboration and the incorporation among the multiple UAV swarm networking.

VI. EVALUATION

In this section, we will present our evaluation of optimization on throughput among the multiple heterogeneous UAS swarm networking. The evaluation is executed on Matlab 2019b and the configuration of the workstation is as the following. CPU: E5-1607; OS: Ubuntu 18.04 LTS.

The configuration is shown as TABLE I. In this evaluation, each UAS is installed with compact 5G NR devices and the carrier is 28 GHz with one beam enabled. To simulate the practical dynamics of UAV swarm networking, we deploy 1000 UAS in three heterogeneous swarms with the constraint of the oval space randomness in Poisson distribution ($\lambda = 20$) respectively. Swarm A, swarm B, swarm C follow the spatial constraints: $\frac{x^2}{(a-b)x+ab} + \frac{y^2+z^2}{c^2} = 1$. a=20~m,~b=30~m,~c=25~m in the space constraint: $100~m \times 200~m \times 100~m$.

Fig. 4 shows the min throughput for each separated networking including two cell walls. As the range of beams generated from 5G NR devices increases, the min throughput escalates correspondingly for each networking. The min throughput of cell walls is lower than the inner throughput of UAV swarms. From our observation, the active links in UAV swarms are higher than cell wall construction. Compared with cell wall

TABLE I 5G NR INSTALLMENT CONFIGURATION

Transmission Power, p	20 dBm
Distances between centers of UAV swarm, d	80 m
Direct gain, g	30 dB
Carrier frequency, f	28 GHz
Noise power, N_0/B	-174 dBm/Hz
Bandwidth	1~GHz
Minimum SINR threshold	-5 dB

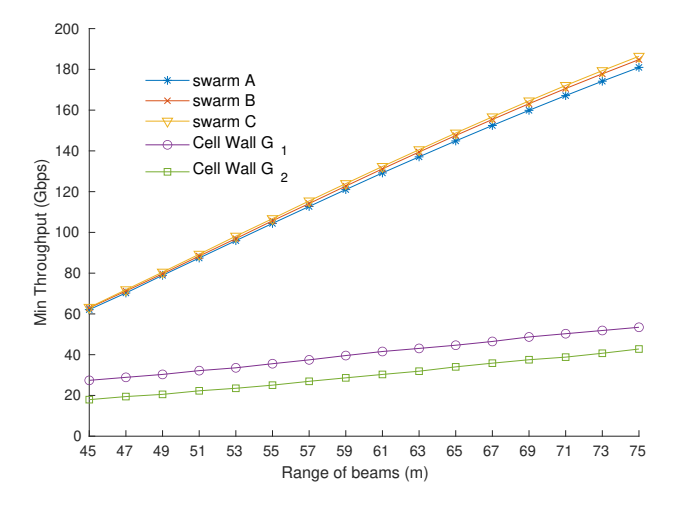


Fig. 4. Min throughput of cell wall and swarm networking

 G_1 , there are more conflicts on the cell wall G_2 so that the min throughput for cell wall G_2 is less than cell wall G_1 .

Fig. 5 shows the max-min throughput for each separated networking. With Algorithm 1, we optimize the active links with the maximization of capacities of the active links set. The normalized throughput enhancement shows that cell wall G_1 and cell wall G_2 improved significantly which is around $38\% \sim 44\%$. Less than cell wall G_1 and cell wall G_2 , swarm A, swarm B, and swarm C keep stable enhancement at around $24\% \sim 25\%$.

Fig.6 shows t_g enhancement of throughput for UAV swarm networking and cell walls. With adjustment of t_g , we can

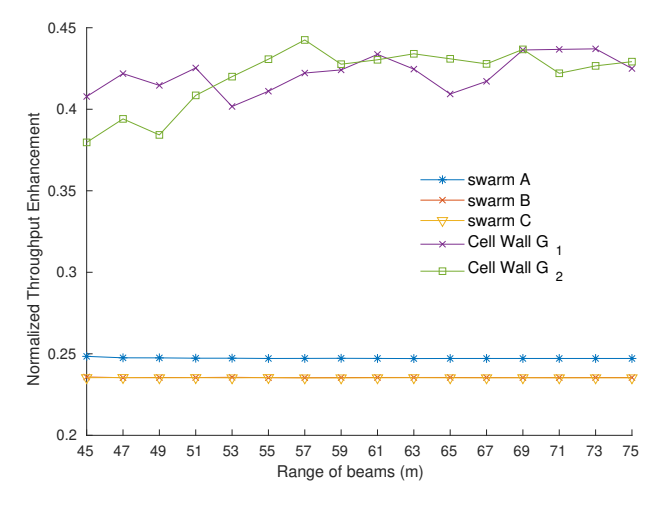


Fig. 5. Max-min throughput of cell wall and swarm networking

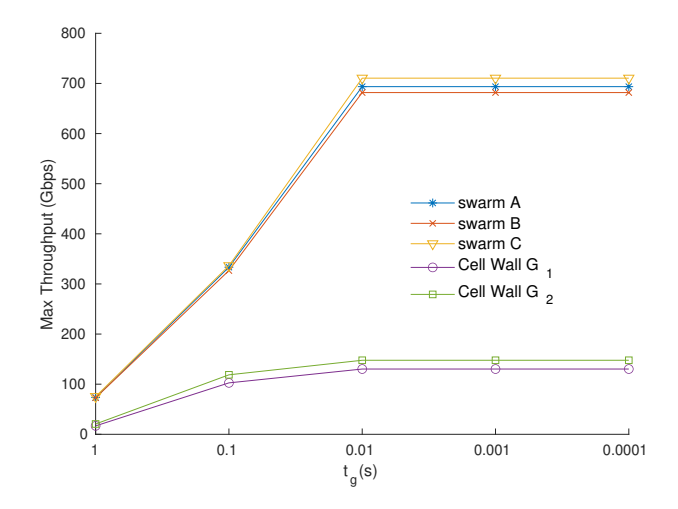


Fig. 6. t_g enhancement of throughput

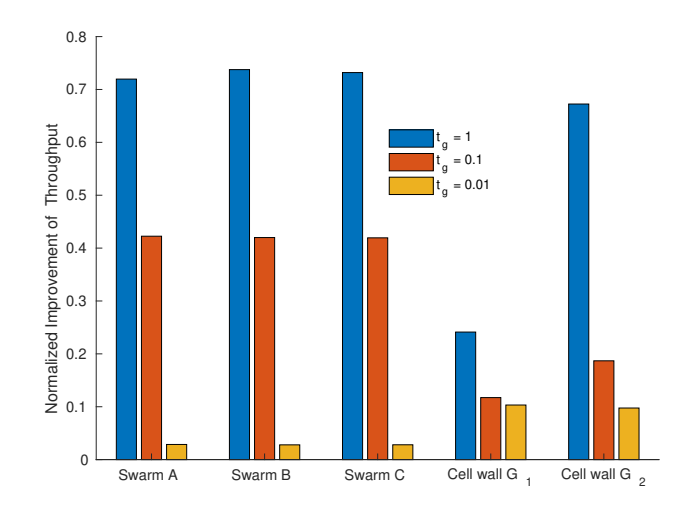


Fig. 7. Optimized scheduling of t_g

obtain the max throughput of each separate networking which is based on the max-min throughput improvement. As t_g increases, we can observe that the max throughput escalates at the same time. Swarm A, swarm B, and swarm C show the same inclining trend with the extension of t_g which is much higher than the enhancement of cell wall G_1 and G_2 . When the t_g is less than 0.01s, the max throughput of all networking keeps stable as the maximization of the specific networking.

Fig. 7 shows the optimization of scheduling on the achievement of t_g . Based on the conclusion of Fig. 6, we mainly attain the optimization of scheduling on $t_g = \{1s, 0.1s, 0.01s\}$. In these tree situations, we leverage the edge coloring with P to obtain the optimized scheduling of the networking. As Fig. 7 shows, we can find that the optimized enhancement on t_g is prominent. Apart from cell wall G_1 , all networking are improved over 60% when $t_g = 1s$. Especially, swarm B can achieve the maximal improvement at 73.8%.

Compared with cell wall G_2 , cell wall G_1 shows slightly enhancement when $t_g=1s$ and weak optimizations when $t_g=0.1s$ and $t_g=0.01s$.

Fig. 8 shows the optimal throughput on the intra intervals and the inter intervals. The combination of t_q and t_s shows the

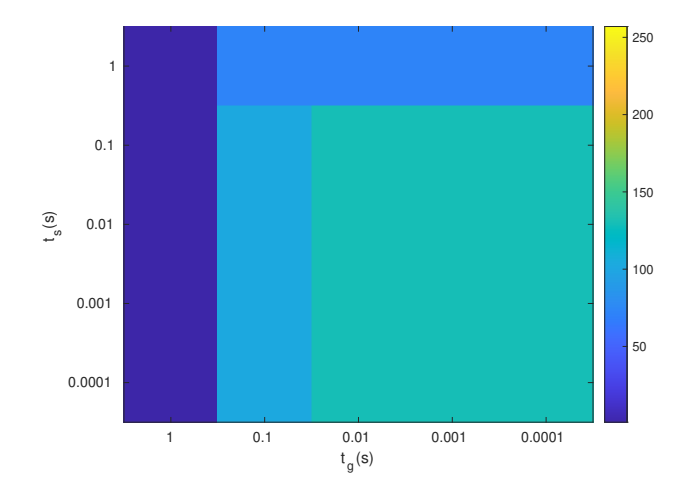


Fig. 8. Max balance throughput of inter and intra swarm networking

optimal throughput from swarm A to swarm C with two cell walls $(G_1 \text{ and } G_2)$. When both t_g and t_s are less than 0.01s the throughput of the heterogeneous UAV swarms can be achieved globally. When t_g is less than 1s, we can obtain the local optimization for each UAV swarm networking. However, only t_s is less than t_g , the local optimization can be guaranteed.

VII. CONCLUSION

In this paper, inspired with cell communication, we propose a cell wall construction for the inter communication between heterogeneous UAV swarm networking to escalate the feasibility and the throughput for the heterogeneous UAV swarm networking. To improve the throughput of heterogeneous UAV swarm networking, we formulate the optimization of the heterogeneous UAV swarm networking into an edge coloring problem. Compared with the conventional edge coloring problem, we propose an optimal edge coloring solution and enhance it. With collision mitigation, we can attain an optimal allocation of time for each channel in the connection derived from heterogeneous UAV swarm networking. The evaluation shows that the proposed approaches can reduce the time slots generation and extend the connections between heterogeneous UAV swarm networking. Compared with the hierarchical and the central architectures we can obtain more robust and feasible throughput for the communication between the heterogeneous UAV swarm networking. Our work can pave a way for the deployment of UAV swarm networking and the massive collaboration and cooperation of UAV swarm networking on a large scale with variable mission allocations.

ACKNOWLEDGMENT

This work was supported in part by the National Science Foundation under Grant No. 1956193.

REFERENCES

- [1] X. Yue, Y. Liu, J. Wang, H. Song, and H. Cao, "Software defined radio and wireless acoustic networking for amateur drone surveillance," *IEEE Communications Magazine*, vol. 56, no. 4, pp. 90–97, 2018.
- [2] E. Liu, E. Effiok, and J. Hitchcock, "Survey on health care applications in 5g networks," *IET Communications*, vol. 14, no. 7, pp. 1073–1080, 2020.

- [3] A. Eid, X. He, R. Bahr, T. H. Lin, Y. Cui, A. Adeyeye, B. Tehrani, and M. M. Tentzeris, "Inkjet-/3d-/4d-printed perpetual electronics and modules: Rf and mm-wave devices for 5g+, iot, smart agriculture, and smart cities applications," *IEEE Microwave Magazine*, vol. 21, no. 12, pp. 87–103, 2020.
- [4] R. Ma, K. H. Teo, S. Shinjo, K. Yamanaka, and P. M. Asbeck, "A gan pa for 4g lte-advanced and 5g: Meeting the telecommunication needs of various vertical sectors including automobiles, robotics, health care, factory automation, agriculture, education, and more," *IEEE Microwave Magazine*, vol. 18, no. 7, pp. 77–85, 2017.
- [5] J. Wang, Y. Liu, S. Niu, and H. Song, "Beamforming-constrained swarm uas networking routing," *IEEE Transactions on Network Science and Engineering*, pp. 1–1, 2020.
- [6] P. Dinh, T. M. Nguyen, S. Sharafeddine, and C. Assi, "Joint location and beamforming design for cooperative uavs with limited storage capacity," *IEEE Transactions on Communications*, vol. 67, no. 11, pp. 8112–8123, 2019.
- [7] D. Liu, Y. Xu, J. Wang, J. Chen, Q. Wu, A. Anpalagan, K. Xu, and Y. Zhang, "Opportunistic utilization of dynamic multi-uav in deviceto-device communication networks," *IEEE Transactions on Cognitive Communications and Networking*, vol. 6, no. 3, pp. 1069–1083, 2020.
- [8] K. Yao, J. Wang, Y. Xu, Y. Xu, Y. Yang, Y. Zhang, H. Jiang, and J. Yao, "Self-organizing slot access for neighboring cooperation in uav swarms," *IEEE Transactions on Wireless Communications*, vol. 19, no. 4, pp. 2800–2812, 2020.
- [9] D. Fan, F. Gao, B. Ai, G. Wang, Z. Zhong, Y. Deng, and A. Nallanathan, "Channel estimation and self-positioning for uav swarm," *IEEE Transactions on Communications*, vol. 67, no. 11, pp. 7994–8007, 2019.
- [10] H. El Hammouti, M. Benjillali, B. Shihada, and M. Alouini, "Learn-as-you-fly: A distributed algorithm for joint 3d placement and user association in multi-uavs networks," *IEEE Transactions on Wireless Communications*, vol. 18, no. 12, pp. 5831–5844, 2019.
- [11] A. M. Koushik, F. Hu, and S. Kumar, "Deep Q -learning-based node positioning for throughput-optimal communications in dynamic uav swarm network," *IEEE Transactions on Cognitive Communications and Networking*, vol. 5, no. 3, pp. 554–566, 2019.
- [12] Y. Han, L. Liu, L. Duan, and R. Zhang, "Towards reliable uav swarm communication in d2d-enhanced cellular network," *IEEE Transactions* on Wireless Communications, pp. 1–1, 2020.
- [13] S. Zhang, H. Zhang, B. Di, and L. Song, "Cellular uav-to-x communications: Design and optimization for multi-uav networks," *IEEE Transactions on Wireless Communications*, vol. 18, no. 2, pp. 1346–1359, 2019.
- [14] M. Mozaffari, A. Taleb Zadeh Kasgari, W. Saad, M. Bennis, and M. Debbah, "Beyond 5g with uavs: Foundations of a 3d wireless cellular network," *IEEE Transactions on Wireless Communications*, vol. 18, no. 1, pp. 357–372, 2019.
- [15] P. Wang, C. Chen, S. Kumari, M. Shojafar, R. Tafazolli, and Y. Liu, "Hdma: Hybrid d2d message authentication scheme for 5g-enabled vanets," *IEEE Transactions on Intelligent Transportation Systems*, pp. 1–10, 2020.
- [16] M. M. Azari, F. Rosas, and S. Pollin, "Cellular connectivity for uavs: Network modeling, performance analysis, and design guidelines," *IEEE Transactions on Wireless Communications*, vol. 18, no. 7, pp. 3366–3381, 2019.
- [17] M. M. Azari, G. Geraci, A. Garcia-Rodriguez, and S. Pollin, "Uav-to-uav communications in cellular networks," *IEEE Transactions on Wireless Communications*, vol. 19, no. 9, pp. 6130–6144, 2020.
- [18] M. A. Ali and A. Jamalipour, "Uav placement and power allocation in uplink and downlink operations of cellular network," *IEEE Transactions* on Communications, vol. 68, no. 7, pp. 4383–4393, 2020.
- [19] J. Ji, K. Zhu, D. Niyato, and R. Wang, "Probabilistic cache placement in uav-assisted networks with d2d connections: Performance analysis and trajectory optimization," *IEEE Transactions on Communications*, vol. 68, no. 10, pp. 6331–6345, 2020.
- [20] M. Chen, W. Saad, and C. Yin, "Liquid state machine learning for resource and cache management in Ite-u unmanned aerial vehicle (uav) networks," *IEEE Transactions on Wireless Communications*, vol. 18, no. 3, pp. 1504–1517, 2019.
- [21] T. Hou, Y. Liu, Z. Song, X. Sun, and Y. Chen, "Multiple antenna aided noma in uav networks: A stochastic geometry approach," *IEEE Transactions on Communications*, vol. 67, no. 2, pp. 1031–1044, 2019.
- [22] K. Wang, P. Xu, C. M. Chen, S. Kumari, M. Shojafar, and M. Alazab, "Neural architecture search for robust networks in 6g-enabled massive iot domain," *IEEE Internet of Things Journal*, pp. 1–1, 2020.

- [23] D. Zhai, H. Li, X. Tang, R. Zhang, Z. Ding, and F. R. Yu, "Height optimization and resource allocation for noma enhanced uav-aided relay networks," *IEEE Transactions on Communications*, pp. 1–1, 2020.
- [24] F. Cui, Y. Cai, Z. Qin, M. Zhao, and G. Y. Li, "Multiple access for mobile-uav enabled networks: Joint trajectory design and resource allocation," *IEEE Transactions on Communications*, vol. 67, no. 7, pp. 4980–4994, 2019.
- [25] T. Hou, Y. Liu, Z. Song, X. Sun, and Y. Chen, "Exploiting noma for uav communications in large-scale cellular networks," *IEEE Transactions on Communications*, vol. 67, no. 10, pp. 6897–6911, 2019.
- [26] N. Zhao, F. Cheng, F. R. Yu, J. Tang, Y. Chen, G. Gui, and H. Sari, "Caching uav assisted secure transmission in hyper-dense networks based on interference alignment," *IEEE Transactions on Communica*tions, vol. 66, no. 5, pp. 2281–2294, 2018.
- [27] T. Zhang, Y. Wang, Y. Liu, W. Xu, and A. Nallanathan, "Cache-enabling uav communications: Network deployment and resource allocation," *IEEE Transactions on Wireless Communications*, vol. 19, no. 11, pp. 7470–7483, 2020.
- [28] Y. Sun, Z. Ding, and X. Dai, "A user-centric cooperative scheme for uavassisted wireless networks in malfunction areas," *IEEE Transactions on Communications*, vol. 67, no. 12, pp. 8786–8800, 2019.
- [29] J. Wang, Y. Liu, and H. Song, "Counter-unmanned aircraft system(s) (c-uas): State of the art, challenges, and future trends," *IEEE Aerospace and Electronic Systems Magazine*, vol. 36, no. 3, pp. 4–29, 2021.
- [30] C. Zhan and Y. Zeng, "Aerial–ground cost tradeoff for multi-uav-enabled data collection in wireless sensor networks," *IEEE Transactions on Communications*, vol. 68, no. 3, pp. 1937–1950, 2020.
- [31] W. Yi, Y. Liu, Y. Deng, and A. Nallanathan, "Clustered uav networks with millimeter wave communications: A stochastic geometry view," *IEEE Transactions on Communications*, vol. 68, no. 7, pp. 4342–4357, 2020
- [32] H. Wang, Y. Zhang, X. Zhang, and Z. Li, "Secrecy and covert communications against uav surveillance via multi-hop networks," *IEEE Transactions on Communications*, vol. 68, no. 1, pp. 389–401, 2020.
- [33] H. Li and X. Zhao, "Throughput maximization with energy harvesting in uav-assisted cognitive mobile relay networks," *IEEE Transactions on Cognitive Communications and Networking*, pp. 1–1, 2020.
- [34] M. Monemi and H. Tabassum, "Performance of uav-assisted d2d networks in the finite block-length regime," *IEEE Transactions on Communications*, vol. 68, no. 11, pp. 7270–7285, 2020.
- [35] Y. L. Che, Y. Lai, S. Luo, K. Wu, and L. Duan, "Uav-aided information and energy transmissions for cognitive and sustainable 5g networks," *IEEE Transactions on Wireless Communications*, pp. 1–1, 2020.
- [36] M. Garcia, T. Gilbert, and R. Bruno, "Recent updates to the surveillance broadcast services (sbs) system," in 2011 Integrated Communications, Navigation, and Surveillance Conference Proceedings, 2011, pp. 1–45.
- [37] B. Jiang, J. Yang, H. Xu, H. Song, and G. Zheng, "Multimedia data throughput maximization in internet-of-things system based on optimization of cache-enabled uav," *IEEE Internet of Things Journal*, vol. 6, no. 2, pp. 3525–3532, 2019.
- [38] W. Debus and L. Axonn, "Rf path loss & transmission distance calculations," Axonn, LLC, 2006.
- [39] H. J. Karloff and D. B. Shmoys, "Efficient parallel algorithms for edge coloring problems," *Journal of Algorithms*, vol. 8, no. 1, pp. 39 – 52, 1987. [Online]. Available: http://www.sciencedirect.com/science/article/ pii/0196677487900265
- [40] J. Gilbert, "Strategies for multigraph edge coloring," *Johns Hopkins APL Technical Digest (Applied Physics Laboratory)*, vol. 23, pp. 187–201, 04 2002.



Jian Wang is a Ph.D. candidate in the Department of Electrical Engineering and Computer Science, Embry-Riddle Aeronautical University (ERAU), Daytona Beach, Florida, and a graduate research assistant in the Security and Optimization for Networked Globe Laboratory (SONG Lab, www.SONGLab.us). He received his M.S. from South China Agricultural University in 2017 and B.S. from Nanyang Normal University in 2014. His major research interests include wireless networks, unmanned aircraft systems, and machine learning.



Yongxin Liu received his B.S. and M.S. from SCAU in 2011 and 2014, respectively, and he received Ph.D. from the School of Civil Engineering and Transportation, South China University of Technology. His major research interests include data mining, wireless networks, the Internet of Things, and unmanned aerial vehicles.



processing.

Shuteng Niu is a Ph.D. candidate in the Department of Electrical Engineering and Computer Science, Embry-Riddle Aeronautical University (ERAU), Daytona Beach, Florida, and a graduate research assistant in the Security and Optimization for Networked Globe Laboratory (SONG Lab, www.SONGLab.us). He received his M.S. from Embry-Riddle Aeronautical University (ERAU) in 2018 and B.S. from Civil Aviation University of China (CAUC) in 2015. His major research interests include machine learning, data mining, and signal



Houbing Song (M'12–SM'14) received the Ph.D. degree in electrical engineering from the University of Virginia, Charlottesville, VA, in August 2012.

In August 2017, he joined the Department of Electrical Engineering and Computer Science, Embry-Riddle Aeronautical University, Daytona Beach, FL, where he is currently an Assistant Professor and the Director of the Security and Optimization for Networked Globe Laboratory (SONG Lab, www.SONGLab.us). He has served as an Associate Technical Editor for IEEE Communications Maga-

zine (2017-present), an Associate Editor for IEEE Internet of Things Journal (2020-present) and IEEE Journal on Miniaturization for Air and Space Systems (J-MASS) (2020-present), and a Guest Editor for IEEE Journal on Selected Areas in Communications (J-SAC), IEEE Internet of Things Journal, IEEE Transactions on Industrial Informatics, IEEE Sensors Journal, IEEE Transactions on Intelligent Transportation Systems, and IEEE Network. He is the editor of six books, including Big Data Analytics for Cyber-Physical Systems: Machine Learning for the Internet of Things, Elsevier, 2019, Smart Cities: Foundations, Principles and Applications, Hoboken, NJ: Wiley, 2017, Security and Privacy in Cyber-Physical Systems: Foundations, Principles and Applications, Chichester, UK: Wiley-IEEE Press, 2017, Cyber-Physical Systems: Foundations, Principles and Applications, Boston, MA: Academic Press, 2016, and Industrial Internet of Things: Cybermanufacturing Systems, Cham, Switzerland: Springer, 2016. He is the author of more than 100 articles. His research interests include cyber-physical systems, cybersecurity and privacy, internet of things, edge computing, AI/machine learning, big data analytics, unmanned aircraft systems, connected vehicle, smart and connected health, and wireless communications and networking. His research has been featured by popular news media outlets, including IEEE GlobalSpec's Engineering360, USA Today, U.S. News & World Report, Fox News, Association for Unmanned Vehicle Systems International (AUVSI), Forbes, WFTV, and New Atlas.

Dr. Song is a senior member of ACM and an ACM Distinguished Speaker. Dr. Song was a recipient of the Best Paper Award from the 12th IEEE International Conference on Cyber, Physical and Social Computing (CPSCom-2019), the Best Paper Award from the 2nd IEEE International Conference on Industrial Internet (ICII 2019), the Best Paper Award from the 19th Integrated Communication, Navigation and Surveillance technologies (ICNS 2019) Conference, the Best Paper Award from the 6th IEEE International Conference on Cloud and Big Data Computing (CBDCom 2020), and the Best Paper Award from the 15th International Conference on Wireless Algorithms, Systems, and Applications (WASA 2020).